CPM Specifications Document Aortofemoral Normal:

OSMSC 0110_0000

May 27, 2013

Version 1

Open Source Medical Software Corporation

1. Clinical Significance & Condition

Studying the hemodynamics of the vasculature distal to the abdominal aorta may be important in understanding common diseases in peripheral arteries downstream of the thoracic aorta. Diseases in the peripheral vasculature affect millions of people in the U.S and can have a profound effect on daily quality of life.

Peripheral arterial disease is the build-up of fatty tissue, or atherosclerosis, in lower extremity arteries. By 2001 at least 10 million people in the U.S were estimated to have peripheral arterial disease. The prevalence of peripheral arterial occlusive disease increases with age and can increase to up to 20% of the population in the geriatric population **[1]**. Up to 4 million people in the U.S suffer from intermittent claudication causing pain in the legs during exercise. Atherosclerotic occlusive disease of the lower extremity arteries is a major cause of walking impairment, pain, ulcerations and gangrene.

Renal artery stenosis can have a prevalence of up to 45% in selective populations, specifically populations with other vascular disease. Prevalence can be from 1-6% in hypertensive patients to 30-45% in patients with aortoiliac occlusive disease or abdominal aortic aneurysms [1]. It is most often caused by atherosclerosis in the renal arteries and is often undetected until symptoms become severe. The most common symptom of renal artery stenosis is hypertension, which can have significant effects on the entire vasculartur. Up to 24% of patients with renal insuffiency, which can lead to end-stage renal disease renal disease, had renal artery stenosis, suggesting that renal artery stenosis may play an important role in kidney failure [1].

2. Clinical Data

Patient-specific volumetric image data was obtained to create physiological models and blood flow simulations. Details of the imaging data used can be seen in Table 1. See Appendix 1 for details on image data orientation.

Table 1 – Patient-specific volumetric image data details (mm). Voxel Spacing, voxel dimensions, and physical dimensions are provided in the Right-Left (R), Anterior-Posterior (A), and Superior-Inferior (S) direction.

OSMSC ID	Modality	Voxel Spacing			Voxel Dimensions			Physical Dimensions		
		R	A	S	R	A	S	R	A	S
0110_0000	MR	0.7813	2.0000	0.7813	512	64	512	400	128	400

No patient specific clinical data other than age and gender were available for patient 0110_0000. This information can be found in Table 2

Table 2 – Available patient-specific clinical data

OSMSC ID	Age	Gender
0110_0000	67	M

Details on available PCMRI can be seen in Table 3.

Table 3 – Available PCMRI

ID	Slice Location	Number of Frames	Voxel Spacing (mm)	
			X	Y
0110_0000	aorta_above_celiac_SMA_2	18	1.5625	1.5625
	celiac_SMA	18	1.5625	1.5625
	right_renals	18	1.5625	1.5625
	left_renals	18	1.5625	1.5625
	aorta_below_renals	18	1.5625	1.5625
	aorta_above_IMA	18	1.5625	1.5625
	aorta_below_IMA	18	1.5625	1.5625
	right_iliac	18	1.5625	1.5625
	left_iliac	18	1.5625	1.5625

3. Anatomic Model Description

Anatomic models were created using customized SimVascular software (Simtk.org) and the image data described in Section 2. The aortofemoral model extends from the supraceliac aorta to the femoral and profunda femoris artery bifurcation. See

Table 4 for a visual summary of the image data, paths, segmentations and solid model constructed.

Table 4 – Visual summary of image data, paths, segmentations and solid model.

OSMSC ID	Image Data	Paths	Paths and Segmentations	Model
ID: OSMSC0110 subID: 0000 Age: 67 Gender: M	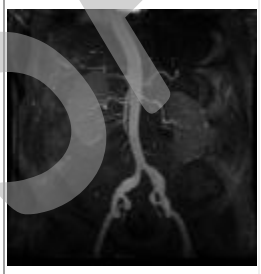	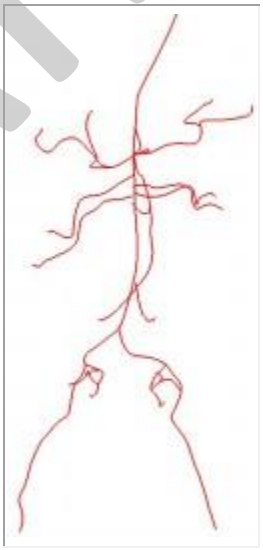	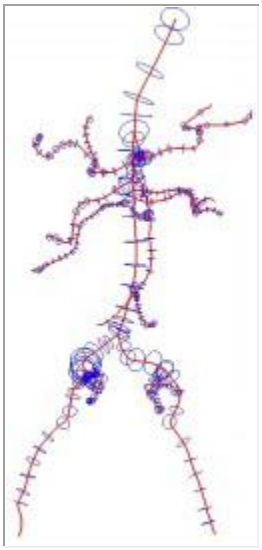	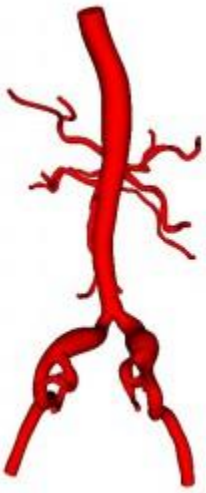

Details of anatomic models, such has number of outlets and model volume, can be seen in Table 5.

Table 5 – Anatomic Model details

OSMSC ID	Inlets	Outlets (cm^3)	Volume (cm^2)	Surface Area (cm^2)	Vesel Paths	2-D Segementations
0110_0000	1	19	182.581	548.575	19	300

4. Physiological Model Description

In addition to the clinical data gathered for this model, several physiological assumptions were made in preparation for running the simulation. See Appendix 3 for details.

5. Simulation Parameters & Details

5. 1 Simulation Parameters

See Appendix 4 for information on the physiology and simulation specifications. For simulation parameters see Table 6.

Table 6- Simulation Parameters

OSMSC ID	Time Steps per Cycle	Time Stepping Strategy
0110_0000	3200	fixed_step 3

5. 2 Inlet Boundary Conditions

A supraceliac aorta blood flow waveform derived from PC-MRI data was prescribed to the inlet of the computational fluid dynamics (CFD) model (Figure 1). See Table 7 for the period and cardiac output for each simulation. Note that the cardiac output is not the same as the supraceliac flow, or the flow prescribed at the inlet. The flow to the supraceliac aorta from PC-MRI was 4.04 L/min.

Table 7 – Period and Cardiac Output from waveforms seen in Figure 1

OSMSC ID	Period (s)	Cardiac Output (L/min)	Profile Type
0110_0000	0.75	6.12	Womersley

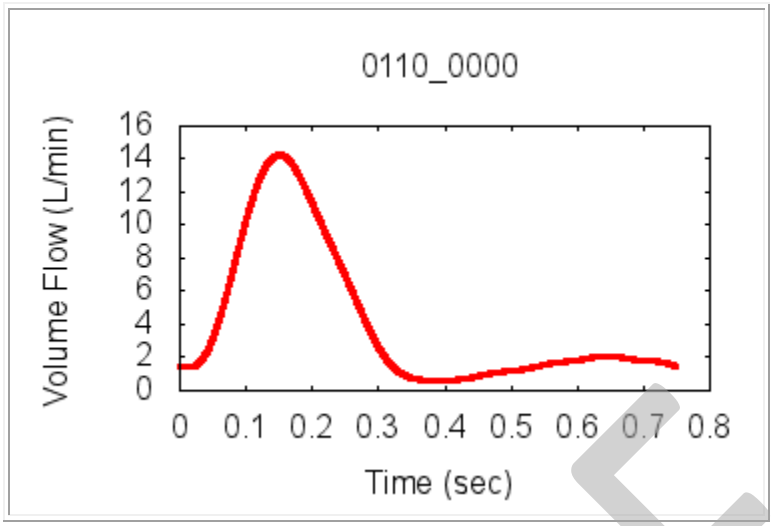

Figure 1 – Inflow waveforms in L/min

5. 3 Outlet Boundary Conditions

A three element Windkessel model was applied at each outlet. For more information refer to Exhibit 1 and Appendix 5. To define the parameters in the Windkessel model the mean flow to each outlet were calculated from PC-MRI data. PCMRI data was available transverse to the celiac trunk, SMA, right superior and inferior renal arteries, left superior and inferior renal arteries, infrarenal aorta, supra-IMA aorta, infra-IMA aorta, right common iliac, and left common iliac. For larger arteries (i.e. supraceliac, infrarenal, supra-IMA and infra-IMA aorta), manual or threshold intensity magnitude segmentation techniques were used to calculate the flow. For medium-sized arteries (i.e. celiac trunk, SMA, left iliac and right iliac), maximum number of intensity pixels were included in PCMRI segmentations to calculate flow. For smaller arteries (i.e. renal arteries), pixels within the artery lumen that form reasonable flow waveforms were hand-picked and tagged to calculate flow. The supraceliac aortic flow, also calculated from PC-MRI, was assumed to be 66% of the cardiac output. Flows calculated from PCMRI were then scaled so that the sum of the flow going to all arteries in the abdominal aorta would equal 66% of the cardiac output. See Table 8 for target flow splits and target pressures used (based on pressure for healthy adult males).

Table 8 – Flow distributions and Pressures

OSMSC ID	0110_0000
hepatic_br1	5.3%
hepatic_br2	3.8%
IMA	5.0%
l_ext_iliac	11.1%
l_inf_renal	9.6%
l_int_iliac	2.0%
l_int_iliac_br1	1.8%
l_int_iliac_br2	0.9%
l_sup_renal	6.0%
r_ext_iliac	11.1%
r_inf_renal	3.6%
r_int_iliac	2.5%
r_int_iliac_br1	1.1%
r_int_iliac_br2	1.1%
r_sup_renal	13.1%
SMA	9.2%
SMA_br1	4.9%
splenic_br1	3.8%
splenic_br2	3.8%
Diastolic Pressure (mmHg)	78
Mean Pressure (mmHg)	94
Ssytolic Pressure (mmHg)	117

6. Simulation Results

Simulation results were quantified for the last cardiac cycle. Paraview (Kitware, Clifton Park, NY), an open-source scientific visualization application, was used to visualize the results. A volume rendering of velocity magnitude for three time points during the cardiac cycle can be seen in Table 9.

Table 9 – Volume rendering velocity during peak systole, end systole, and end diastole. All renderings have the scale below with units of cm/s

OSMSC ID	Peak Systole	End Systole	End Diastole
ID: OSMSC0110 subID: 0000 Age: 67 Gender: M	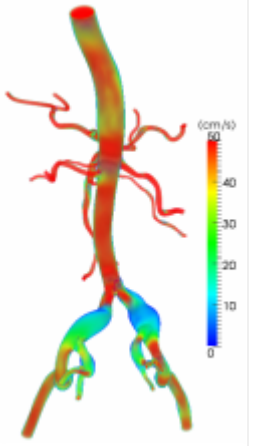	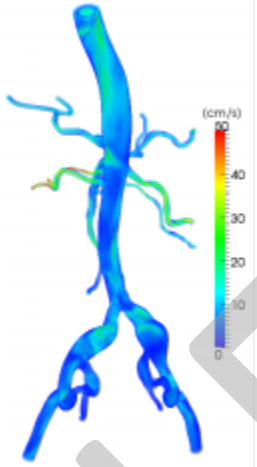	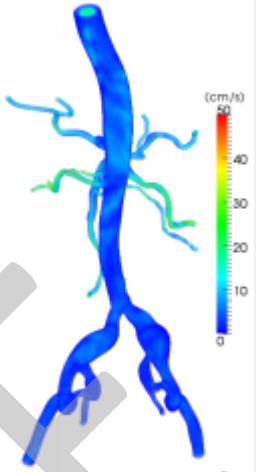

Surface distribution of time-averaged blood pressure (TABP), time-averaged wall shear stress (TAWSS) and oscillatory shear index (OSI) were also visualized and can be seen in Table 10.

Table 10 – Time averaged blood pressure (TABP), time-average wall shear stress (TAWSS), and oscillatory shear index (OSI) surface distributions

OSMSC ID	TABP	TAWSS	OSI
ID: OSMSC0110 subID: 0000 Age: 67 Gender: M	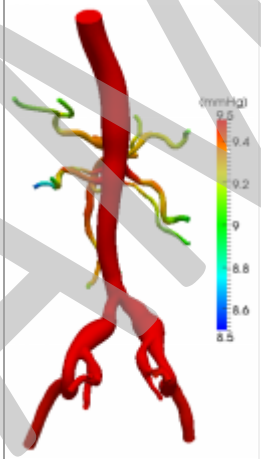	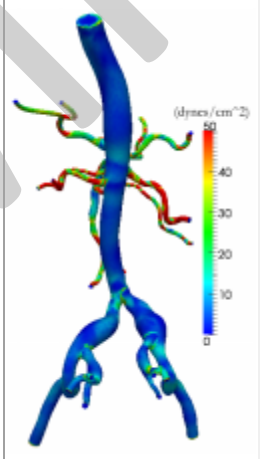	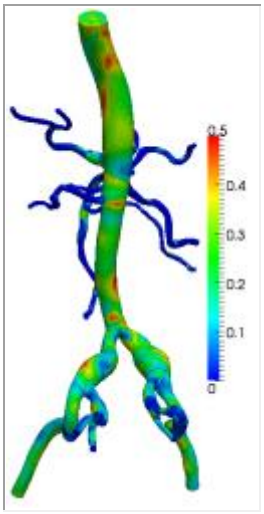

7. References

[1] W. R. Hiatt, A. T. Hirsch and J. Regensteiner, Peripheral Artery Disease Handbook, Boca Raton, FL: CRC Press LLC, 2001.

Exhibit 1: Aortofemoral Simulation RCR Values

Information on how RCR values were obtained is included in Appendix 5. RCR values for the final simulations are shown on Table 11.

Table 11 – RCR Values for 0110_0000

Solver ID	Face Name	Rp	C	Rd
2	splenic_br1	2096.02	0.0000260	45005.00
3	splenic_br2	2095.96	0.0000260	44904.30
4	hepatic_br1	1511.53	0.0000360	32383.60
5	hepatic_br2	2095.59	0.0000260	45243.00
6	SMA	867.84	0.0000627	18429.90
7	SMA_br1	1617.35	0.0000337	35259.30
8	R_sup_renal	609.70	0.0000893	12991.00
9	R_inf_renal	2222.74	0.0000245	47359.60
10	L_sup_renal	1330.80	0.0000408	27260.40
11	L_inf_renal	829.38	0.0000656	17593.90
12	IMA	1583.13	0.0000344	34215.40
13	R_ext_iliac	718.27	0.0000760	15945.20
14	R_int_iliac	3169.51	0.0000172	70363.10
15	R_int_iliac_br1	7094.64	0.0000077	157504.00
16	R_int_iliac_br2	7130.80	0.0000076	158139.00
17	L_ext_iliac	718.27	0.0000760	15945.20
18	L_int_iliac	3903.05	0.0000140	86649.70
19	L_int_iliac_br1	4424.33	0.0000123	98323.60
20	L_int_iliac_br2	8737.84	0.0000062	193983.00

Appendix

1. Image Data Orientation

The RAS coordinate system was assumed for the image data orientation. Voxel Spacing, voxel dimensions, and physical dimensions are provided in the Right-Left (R), Anterior-Posterior (A), and Superior-Inferior (S) direction in all specification documents unless otherwise specified.

2. Model Construction

All anatomic models were constructed in RAS Space. The models are generated by selecting centerline paths along the vessels, creating 2D segmentations along each of these paths, and then lofting the segmentations together to create a solid model. A separate solid model was created for each vessel and Boolean addition was used to generate a single model representing the complete anatomic model. The vessel junctions were then blended to create a smoothed model.

3. Physiological Assumptions

Newtonian fluid behavior is assumed with standard physiological properties. Blood viscosity and density are given below in units used to input directly into the solver.

Blood Viscosity: 0.04 g/cm•s^2
Blood Density: 1.06 g/cm^3

4. Simulation Parameters

Conservation of mass and Navier-Stokes equations were solved using 3D finite element methods assuming rigid and non-slip walls. All simulations were ran in cgs units and ran for several cardiac cycles to allow the flow rate and pressure fields to stabilize.

5. Outlet Boundary Conditions

5.1 Resistance Methods

Resistances values can be applied to the outlets to direct flow and pressure gradients. Total resistance for the model is calculated using relationships of the flow and pressure of the model. Total resistance is than distributed amongst the outlets using an inverse relationship of outlet area and the assumption that the outlets act in parallel.

5.2 Windkessel Model

In order to represent the effects of vessels distal to the CFD model, a three-element Windkessel model can be applied at each outlet. This model consists of proximal resistance (R_p), capacitance (C), and distal resistance (R_d) representing the resistance of the proximal vessels, the capacitance of the proximal vessels, and the resistance of the distal vessels downstream of each outlet, respectively (Figure 1).

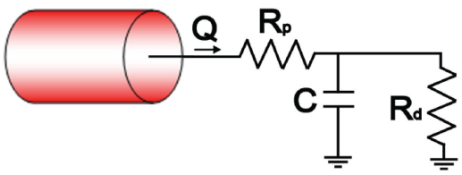

Figure 2 - Windkessel model

First, total arterial capacitance (TAC) was calculated using inflow and blood pressure. The TAC was then distributed among the outlets based on the blood flow distributions. Next, total resistance (R_t) was calculated for each outlet using mean blood pressure and PC-MRI or calculated target flow ($R_t=P_{mean}/Q_{desired}$). Given that $R_t=R_p+R_d$, total resistance was distributed between R_p and R_d adjusting the R_p to R_t ratio for each outlet.